
Monotonic Transformation Invariant Multi-task Learning

Surya Murthy^{*1} Kushagra Gupta^{*1} Mustafa Karabag¹ David Fridovich-Keil¹ Ufuk Topcu¹

Abstract

Multi-task learning (MTL) algorithms typically rely on schemes that combine different task losses or their gradients through weighted averaging. These methods aim to find Pareto stationary points by using heuristics that require access to task loss values, gradients, or both. In doing so, a central challenge arises because task losses can be arbitrarily scaled relative to one another, causing certain tasks to dominate training and degrade overall performance. A recent advance in cooperative bargaining theory, the Direction-based Bargaining Solution (DiBS), yields Pareto stationary solutions immune to task domination because of its invariance to monotonic nonaffine task loss transformations. However, the convergence behavior of DiBS in nonconvex MTL settings is currently not understood. To this end, we prove that under standard assumptions, a subsequence of DiBS iterates converges to a Pareto stationary point when task losses are nonconvex, and propose DiBS-MTL, an adaptation of DiBS to the MTL setting which is more computationally efficient than prior bargaining-inspired MTL approaches. Finally, we empirically show that DiBS-MTL is competitive with leading MTL methods on standard benchmarks, and it drastically outperforms state-of-the-art baselines in multiple examples with poorly-scaled task losses, highlighting the importance of invariance to non-affine monotonic transformations of the loss landscape. Code available at <https://github.com/suryakmurthy/dibs-ntl>

1. Introduction

The successes of deep learning have inspired investigation into “generalist” networks—models simultaneously trained for learning multiple tasks. As a result, numerous multi-

¹The University of Texas at Austin, TX 78712, USA. Correspondence to: Surya Murthy <surya.murthy@utexas.edu>, Kushagra Gupta <kushagra@utexas.edu>.

Preprint. February 3, 2026.

task learning (MTL) algorithms have been developed to tackle the inevitable conflict between task-specific loss gradients, aiming to ensure that during training, no task is under-optimized compared to others (Kendall et al., 2018; Sener & Koltun, 2018; Yu et al., 2020a; Liu et al., 2021a; Navon et al., 2022; Liu et al., 2023). However, most existing MTL methods are not robust against nonaffine (monotonic) transformations to task losses, which is a crucial property desirable in the context of deep learning—where some preferences can be represented with losses of different nonaffine scalings, and it is unclear which relative scaling of the different losses ensures balanced learning without expensive and exhaustive ablations. We consider the problem of multi-task learning (MTL) through the lens of centralized, cooperative bargaining methods that are invariant to *nonaffine* monotonic task loss transformations.

The issue of different task losses being directly incomparable and scaled in different, nonaffine fashions arises very naturally in many deep learning domains. For instance, reinforcement learning applications demand that a practitioner leverages prior, task-specific domain knowledge to design an effective reward function (Yu et al., 2025). However, in a downstream MTL setting, the loss corresponding to this reward function may dominate (or get dominated by) other task losses. At the same time, the relative performance of a “good” task-specific policy does not change when the corresponding task loss is monotonically transformed, i.e., the transformation does not change the actual underlying preferences over options. *Thus, in an MTL problem, the available task losses can be seen as monotonic, possibly nonaffine, transformations of some underlying set of ideal, unknown task losses that are meaningfully scaled with respect to each other.*

Recent work in MTL has developed a connection with cooperative game theory (Navon et al., 2022). In this setting, each different loss function is a separate agent in a bargaining game, and the idea is to find a balanced Pareto optimum among the agents’ objectives. Classical solutions to these bargaining games (e.g., Nash, as explored by Navon et al. (2022)) are *not* robust to nonaffine monotonic scalings, and only recently has a technique—Direction-based Bargaining Solution (DiBS)—been developed which remains *invariant* to these transformations (Gupta et al., 2025). However, the convergence of DiBS has only been analyzed in settings

with strongly convex losses, and it is unclear to what extent the favorable properties of DiBS will apply in realistic MTL applications where task losses are almost always nonconvex. Inspired by this, we investigate the following:

1. *What theoretical properties can be established for Direction-based Bargaining Solution (DiBS) in the general setting where agent objectives (task losses) can be nonconvex?*

Contribution 1. We show that under standard assumptions, for nonconvex losses, a subsequence of the DiBS iterates converges to a Pareto stationary point asymptotically. Notably, our result does not require the linear independence of task loss gradients at non-Pareto stationary points, an assumption that is required by MTL methods using the Nash bargaining solution to deliver the same asymptotic guarantee (Navon et al., 2022).

2. *Can DiBS readily adapt to MTL applications? If so, how does it compare to existing MTL methods?*

Contribution 2. We extend DiBS to multi-task learning, showing its natural compatibility with existing bargaining-for-learning frameworks. To this end, we propose DiBS-MTL , which adapts DiBS to MTL utilizing local loss approximations, is computationally more efficient than previous bargaining-inspired MTL approaches, and also preserves desirable invariance to nonaffine monotonic task loss transformations. We empirically show that DiBS-MTL performs competitively with state-of-the-art MTL methods on widely used vision and quantum chemistry MTL benchmarks.

Contribution 3. We further investigate settings where task losses are nonaffinely and poorly scaled relative to each other in two domains—a challenging synthetic problem that exhibits substantial nonconvexity (and which highlights Contribution 1), and a larger-scale multi-task reinforcement learning benchmark. We show that DiBS-MTL drastically outperforms state-of-the-art baselines in these domains; highlighting the importance of MTL methods to be invariant to nonaffine monotonic transformations of the loss landscape.

2. On related MTL works and existing bargaining solutions

2.1. Related MTL literature

The most popular MTL approach in practice is linear scalarization (LS)—constructing a scalarized loss by taking the unweighted sum of task losses, or using known static coefficients to compute a weighted average. While previous work has advocated for LS methods (Kurin et al., 2022; Xin et al., 2022), in practice, LS can lead to situations where certain tasks remain under-optimized. Further, it has been

shown that LS also does not necessarily recover the entire Pareto front generated by the task losses (Hu et al., 2023). Other methods tackle the MTL problem through more sophisticated multiobjective optimization approaches, aiming to find Pareto optimal (or stationary, in general nonconvex settings) points. Such methods seek to address the task imbalances arising during training via heuristics that (i) use task-specific loss values to compute a scalar weighted average loss (but with evolving weights, unlike LS) (Kendall et al., 2018; Liu et al., 2019; Lin et al., 2022; Liu et al., 2023), or (ii) use task-specific loss gradients to find update directions iteratively during training (Sener & Koltun, 2018; Yu et al., 2020a; Chen et al., 2020; Liu et al., 2021a;b; Navon et al., 2022).

Existing loss-based heuristics include maximizing improvement of the worst-performing task (Liu et al., 2023), forcing improvements to be similar across tasks (Liu et al., 2019), weighting task losses randomly (Lin et al., 2022), weighting task losses according to relative improvements (Chen et al., 2018), and adapting weights according to task-based uncertainty measures (Kendall et al., 2018). Heuristics for gradient-based approaches include finding mutual task improvement directions (Yu et al., 2020a), probabilistically masking task gradients according to their sign (Chen et al., 2020), computing weights that minimize the norm of the convex combination of task gradients (Sener & Koltun, 2018), using gradient-based approaches to maximize improvement of the worst-performing task (Liu et al., 2021a), and finding the Nash bargaining solution for a bargaining subproblem (Navon et al., 2022). However, as we empirically demonstrate in Section 5, these *existing methods are not robust to monotonic, nonaffine task loss transformations*, potentially experiencing significant performance drops in such settings. We remark that one gradient-based method, IMTL-G (Liu et al., 2021b), in principle can produce solutions invariant to monotonic nonaffine task loss transformations. However, we show in Appendix C that even for simple convex problems, IMTL-G can converge to Pareto solutions that heavily favor one task over the other.

Finally, we note that other approaches also exist for the MTL problem, such as (i) task clustering, where methods first cluster tasks to reduce conflicts, and then update model training parameters for each cluster (Standley et al., 2020; Fifty et al., 2021; Song et al., 2022; Shen et al., 2024); and (ii) parameter sharing methods, which design neural network architectures consisting of task-specific and task-shared modules/parameters (Kokkinos, 2017; Guo et al., 2020; Gao et al., 2020). These approaches differ from the proposed approach at a fundamental level, in that they try to design a suite of models for the space of tasks, or design MTL model architectures, whereas the proposed approach aims to optimize *a single* model (with a pre-defined architecture), balancing the performance of all tasks.

2.2. Preliminaries on cooperative bargaining games

We provide a brief background of cooperative bargaining theory, which we utilize in our main contribution. A thorough description can be found in classical literature (Thomson, 1994; Narahari, 2014). A centralized bargaining game consists of N agents and a mediator; and $\mathbf{x} \in \mathcal{S} \subseteq \mathbb{R}^n$ denotes the state of the game. We assume the i^{th} agent has a differentiable cost $\ell^i(\mathbf{x}) : \mathcal{S} \rightarrow \mathbb{R}, i \in [N]$. In the context of MTL, every task can be thought of as being represented by one agent, with the agent’s cost being the task loss.

Each agent wants to minimize its cost, and has preferred states $\mathbf{x}^{*,i} \in \arg \min_{\mathbf{x} \in \mathcal{S}} \ell^i(\mathbf{x})$ it wants the game to go towards. For nonconvex costs, this could be a local minimum. The goal of the mediator is to execute a bargaining strategy and find a solution state \mathbf{x}^\dagger . Let $\ell(\mathbf{x}) = [\ell^1(\mathbf{x}), \dots, \ell^N(\mathbf{x})]$. For convenience, we denote such a bargaining game by $\mathcal{B}_{\mathcal{S}}(\ell)$. Numerous bargaining solutions have been proposed in economics literature (Thomson, 1994), each employing different heuristics to find a Pareto optimal point—a point at which no update direction exists, which simultaneously decreases the losses for all agents. In the case when the agent losses $\ell^i(\mathbf{x})$ are nonconvex, a more appropriate goal for the mediator is to find a *Pareto stationary* point, which is a first-order necessary condition for Pareto optimality.

Definition 1 (Pareto stationarity). For $\mathcal{B}_{\mathcal{S}}(\ell)$, a point $\mathbf{x}^\dagger \in \mathcal{S}$ is Pareto stationary if $\exists \beta^i \geq 0, i \in [N]$, such that $\sum_{i \in [N]} \beta^i \nabla_{\mathbf{x}} \ell^i(\mathbf{x}^\dagger) = 0$, and $\sum_{i \in [N]} \beta^i = 1$.

We now highlight the Direction-based Bargaining Solution (DiBS), which we use in our method. For a bargaining game $\mathcal{B}_{\mathcal{S}}(\ell)$, DiBS finds a Pareto stationary point by taking an initial point $\mathbf{x}_1 \in \mathcal{S}$ and running the iterations

$$\begin{aligned} \mathbf{x}_{k+1} &= \mathbf{x}_k - h(\mathbf{x}_k) \\ &:= \mathbf{x}_k - \alpha_k \cdot \sum_{i \in [N]} \left(\|\mathbf{x}_k - \mathbf{x}^{*,i}\|_2 \cdot \frac{\nabla_{\mathbf{x}} \ell^i(\mathbf{x}_k)}{\|\nabla_{\mathbf{x}} \ell^i(\mathbf{x}_k)\|_2} \right). \end{aligned} \quad (1)$$

Remark 1 (Invariance of DiBS). For monotonic, possibly nonaffine transformations h^1, \dots, h^N , let $\mathbf{h}(\ell)(\mathbf{x}) = [h^1(\ell^1(\mathbf{x})), \dots, h^N(\ell^N(\mathbf{x}))]$. Then DiBS produces the same solution for the bargaining games $\mathcal{B}_{\mathcal{S}}(\mathbf{h}(\ell))$ and $\mathcal{B}_{\mathcal{S}}(\ell)$, for the same initial point $\mathbf{x}_1 \in \mathcal{S}$ and sequence of stepsizes $\{\alpha_k\}_{k \geq 0}$. This invariance to monotonic nonaffine transformations is because DiBS only utilizes normalized gradients and locally preferred states, i.e., local minima, both of which do not change under such transformations.

We also note that prior work has used the classical Nash bargaining solution (NBS) (Nash et al., 1950) in the context of MTL (Navon et al., 2022). However, the NBS is invariant to only affine agent (or task) loss transformations, and can change if the agent (or task) losses undergo monotonic nonaffine transformations.

As highlighted in Section 1, the need for MTL methods which are robust to monotonic nonaffine transformations makes it natural to consider incorporating DiBS—which is invariant to such distortions—in an MTL approach. However, since practical MTL problems typically involve nonconvex losses, it is crucial to examine the behavior of DiBS in the nonconvex regime, a setting not yet analyzed in prior work. This serves as our motivation for the next section.

3. What can we say about DiBS in the nonconvex regime?

In this section we establish a convergence guarantee for DiBS in the setting when agent losses can be nonconvex, which is often the case in practical MTL problems. Currently, guarantees only exist for the case when all agents have strongly convex losses, under which DiBS enjoys global asymptotic convergence to a Pareto stationary point (Gupta et al., 2025). We begin by highlighting our assumptions.

Assumption 1. For $\mathcal{B}_{\mathcal{S}}(\ell)$, the set of Pareto stationary points lies in the interior of \mathcal{S} , and all $\mathbf{x}^{*,i}$ exist, are finite, and are also in the interior of \mathcal{S} . The agent costs ℓ^i are differentiable, and bounded below.

Assumption 2 (Relaxed in Section B). The sequence $\{\mathbf{x}_k\}_{k=1}^\infty$ generated by the DiBS iterations given in Equation (1) are bounded, i.e., there is a bounded set $\mathcal{D} \subseteq \mathcal{S}$ such that $\mathbf{x}_k \in \mathcal{D} \forall k \in \mathbb{N}$.

Assumption 1 is standard and ensures that the problem is well posed. Assumption 2 is a temporary assumption that we make for a clear exposition of our arguments while studying convergence of DiBS in nonconvex settings. Assumption 2 makes the DiBS iterates bounded, and we relax this assumption in Section B, showing that standard techniques from dynamical systems theory can be used to ensure DiBS iterates are bounded, forgoing the need for Assumption 2.

We now present our main theorem, the proof of which is in Appendix A.

Theorem 1. Let $\{\mathbf{x}_k\}_{k=1}^\infty$ be the sequence generated by the DiBS algorithm given in Equation (1), for an initial point $\mathbf{x}_1 \in \mathcal{S}$ and stepsizes that follow the Robbins-Monro conditions, i.e., $\sum_k \alpha_k = \infty, \sum_k \alpha_k^2 < \infty$ (Robbins & Monro, 1951). Then, under Assumptions 1 and 2, the sequence $\{\mathbf{x}_k\}_{k=1}^\infty$ has a subsequence that asymptotically converges to a Pareto stationary point \mathbf{x}^\dagger , i.e., $h(\mathbf{x}^\dagger) = 0$.

Theorem 1 establishes that the sequence produced by the DiBS iterates has a subsequence which converges to a Pareto stationary point, even when the agent losses are nonconvex. Note that this result is similar to a guarantee presented for the Nash bargaining solution in prior work

(Navon et al., 2022). However, the existing result in prior work requires the assumption that agents’ loss gradients are linearly independent at all non-Pareto stationary points. It is unclear to what extent realistic MTL problems satisfy this assumption. In comparison, our result does not require such a linear independence assumption.

Algorithm 1 T -step DiBS-MTL

Require: Initial parameters θ_0 , losses $\{\ell^i\}_{i=1}^N$, learning rate η , approximation radius ϵ , step size $\alpha < \epsilon/N$, number of epochs J

for $j = 1$ to J **do**

 Compute normalized gradients $\bar{g}_{j-1}^i = \frac{\nabla_{\theta} \ell^i(\theta_{j-1})}{\|\nabla_{\theta} \ell^i(\theta_{j-1})\|_2}$

 For each i , compute preferred individual parameters inside ϵ -radius: $\theta_j^{*,i} = \theta_{j-1} - \epsilon \bar{g}_{j-1}^i$,

 Set $\theta_{(j-1,0)} \leftarrow \theta_{j-1}$

 // DiBS updates inside

 approximation radius ϵ

for $t = 1$ to T **do**

 Compute DiBS update direction:

$$d_{(j,t)} = \sum_{i \in [N]} \left(\|\theta_{(j-1,t-1)} - \theta_j^{*,i}\|_2 \cdot \bar{g}_{j-1}^i \right)$$

 Update: $\theta_{(j-1,t)} \leftarrow \theta_{(j-1,t-1)} - \alpha d_{(j,t)}$

end for

$\Delta\theta_{j-1} = \theta_{(j-1,T)} - \theta_{(j-1,0)}$

 Update: $\theta_j \leftarrow \theta_{j-1} + \eta \Delta\theta_{j-1}$

end for

return θ_j

4. Adapting DiBS to multi-task learning

We now extend DiBS to the multi-task learning setting. We begin by introducing some notation, and then describe the underlying bargaining game for MTL, which has been proposed in previous work (Navon et al., 2022).

Notation. We use $\mathbf{0}$ to denote a zero vector of appropriate dimensions, and $\mathcal{V}(\mathbf{x}, r)$ denotes a ball of radius r , centered at \mathbf{x} . The vector $\theta \in \mathbb{R}^n$ represents shared task parameters; any additional task-specific parameters are suppressed for notational convenience and do not influence the calculation of θ iterates in this section. j denotes an epoch iteration, whereas t will denote bargaining updates *within* an epoch.

Bargaining for MTL. The goal in MTL is to train a model to perform multiple tasks. Every learning task has an associated task loss $\ell^i(\theta) : \mathbb{R}^n \rightarrow \mathbb{R}$. During training, given parameters θ_j at some epoch $j + 1$, bargaining is iteratively conducted during the epoch to find the next set of parameters $\theta_{j+1} = \theta_j + \eta \Delta\theta_j$ for some learning rate η .

To this end, every task is represented as a distinct bargaining agent with the (minimization) objective being an approxima-

tion of the difference $\ell^i(\theta_j + \eta \Delta\theta_j) - \ell^i(\theta_j)$. We consider a first-order approximation, in line with prior bargaining work for a fair comparison (Navon et al., 2022), with the i^{th} agent’s objective being

$$\min_{\|\Delta\theta_j\|_2 \leq \epsilon} \underbrace{(\nabla_{\theta} \ell^i(\theta_j))^{\top} \Delta\theta_j}_{:= \omega^i(\Delta\theta_j)},$$

where we constrain the update vector $\Delta\theta_j$ to lie in $\mathcal{V}(\mathbf{0}, \epsilon)$, to prevent overshooting caused by large update steps. *Thus, for an MTL problem with N tasks—the bargaining game becomes $\mathcal{B}_{\mathcal{V}(\mathbf{0}, \epsilon)}([\omega^1, \dots, \omega^N])$.*

DiBS for MTL. We now proceed to apply DiBS to the bargaining game $\mathcal{B}_{\mathcal{V}(\mathbf{0}, \epsilon)}([\omega^1, \dots, \omega^N])$. Note that the bargaining game has linear objectives, and thus the normalized gradient

$$\frac{\nabla_{\Delta\theta_j} \omega^i}{\|\nabla_{\Delta\theta_j} \omega^i\|_2} = \frac{\nabla_{\theta} \ell^i(\theta_j)}{\|\nabla_{\theta} \ell^i(\theta_j)\|_2} := \bar{g}_j^i$$

only needs to be computed once at the starting of a bargaining game. Further, the distance of the individual optima from the initial point in Equation (1) has a closed form solution such that $\Delta\theta_j^{*,i} := \theta_j^{*,i} - \theta_{j-1} = -(\nabla_{\theta} \ell^i(\theta_j) / \|\nabla_{\theta} \ell^i(\theta_j)\|_2) \cdot \epsilon$ for the linear objectives, i.e., an individual optimum is the furthest point in the negative gradient direction, given that $\Delta\theta_j$ is constrained to lie in $\mathcal{V}(\mathbf{0}, \epsilon)$. Thus, for an initial choice $\Delta\theta_{(j,0)} = \mathbf{0}$ and stepsize sequence $\{\alpha_t\}$, T -iterate DiBS for MTL satisfies

$$\Delta\theta_{(j,t+1)} = \Delta\theta_{(j,t)} - \alpha_t \cdot \sum_{i \in [N]} \left(\|\Delta\theta_{(j,t)} + \epsilon \cdot \bar{g}_j^i\|_2 \cdot \bar{g}_j^i \right) \quad (\text{T-step DiBS-MTL})$$

Using this the parameters between epochs are updated as in Algorithm 1. In practice, single-step versions of such iterative schemes are common (Liu et al., 2023). Such a version described below still *preserves* the desirable invariance to monotonic, nonaffine task loss transformations:

$$\Delta\theta_{(j,1)} = -\epsilon \cdot \sum_{i \in [N]} \bar{g}_j^i \quad (\text{1-step DiBS-MTL})$$

We remark that unlike multi-step variants, *1-step DiBS-MTL does not* have explicit dependencies on the individual optima $\theta_j^{*,i}$ due to the first-order approximation combined with the ball constraint. Further, *1-step DiBS-MTL* does not introduce any additional hyperparameters as the ϵ term is absorbed into the learning rate η . In Sections 5.1, 5.3 and F we provide results showing that the single-step version performs similarly to the multi-step version despite being relatively simpler on a variety of MTL problems.

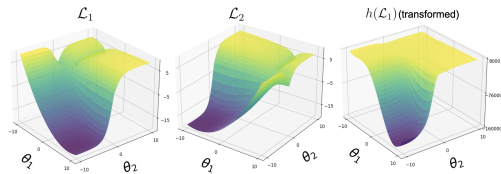


Figure 1. Loss functions in the nonconvex example (Section 5.1). We employ the nonaffine transformation $h(\mathcal{L}_1) = \text{sign}(\mathcal{L}_1) \cdot \mathcal{L}_1^4$.

5. Experiments

We now evaluate DiBS-MTL in standard MTL benchmarks extensively used in literature (Yu et al., 2020a; Liu et al., 2021a; Navon et al., 2022; Liu et al., 2023), a demonstrative two objective example, a multi-task reinforcement learning benchmark (Meta-World MT10) (Yu et al., 2020b), and supervised learning computer vision and graph neural network benchmarks (NYU-v2, Cityscapes and QM9) (Silberman et al., 2012; Cordts et al., 2016; Blum & Reymond, 2009). The results for the Cityscapes benchmark are included in Appendix D. **Our main aims are:** (i) to verify that DiBS-MTL consistently converges to Pareto-optimal solutions from diverse initializations in nonconvex settings, (ii) to show that due to robustness against monotonic nonaffine task loss transformations, DiBS-MTL significantly outperforms state-of-the-art MTL baselines in examples where task losses are poorly scaled relative to each other, and (iii) to confirm that leveraging normalized gradients to achieve this robustness does not compromise the solution quality of DiBS-MTL and that DiBS-MTL is competitive to state-of-the-art baselines across large-scale MTL benchmarks.

5.1. Does DiBS-MTL consistently converge to Pareto solutions from diverse initializations?

Setting. We first test DiBS-MTL on a challenging two-dimensional, nonconvex multi-objective optimization example with two objectives ($\mathcal{L}_1, \mathcal{L}_2$), which is a standard benchmark for illustrating the ability of MTL methods to achieve balanced Pareto solutions (Yu et al., 2020a; Liu et al., 2021a; Navon et al., 2022; Liu et al., 2023; Ban & Ji, 2024). As shown in Figure 1, each objective (provided in Appendix E.1) in this example has deep valleys, with the bottoms having a large magnitude difference between the objective gradients, and a high (positive) curvature. Such phenomenon is documented to exist when optimizing neural networks as well, and can lead to one objective (task) dominating others (Goodfellow et al., 2014; Yu et al., 2020a).

Baselines. We test 5-step DiBS-MTL along with 5 baselines—(1) linear scalarization (LS), which optimizes the unweighted loss average, (2) CAGrad (Liu et al., 2021a), (3) FairGrad (Ban & Ji, 2024), (4) Nash-MTL (Navon

et al., 2022), and (5) FAMO¹ (Liu et al., 2023).

DiBS-MTL yields Pareto solutions from diverse initializations, and unlike other methods, DiBS-MTL is invariant to monotonic nonaffine objective transformations.

Figure 2 plots the solutions generated by DiBS-MTL for different initializations, for the costs ($\mathcal{L}_1, \mathcal{L}_2$) above, as well as for $(h(\mathcal{L}_1), \mathcal{L}_2)$ where we apply the monotonic nonaffine transformation $h(x) = \text{sign}(x) \cdot x^4$ to \mathcal{L}_1 . We observe that DiBS-MTL consistently leads to balanced Pareto solutions for all initializations, and these solutions remain invariant to the transformation. It is also evident that unlike DiBS-MTL, all MTL baselines produce significantly biased solutions once \mathcal{L}_1 is transformed (i.e., comparing the top and bottom rows of Figure 2), signaling that *baselines are susceptible to task domination* when tasks are differently scaled. Further, DiBS-MTL achieves faster runtimes than the previous bargaining-inspired MTL method Nash-MTL (see Section F.1).

5.2. Does the use of normalized gradients in DiBS-MTL induce robustness to nonaffine transformations?

We now conduct experiments in the multi-task reinforcement learning (MTRL) Meta-World MT10 benchmark (Yu et al., 2020b) to investigate how DiBS-MTL and baseline MTL methods perform when some tasks undergo nonaffine transformations. We limit our study in this section to MTRL, because task-specific losses in supervised learning examples such as computer vision are relatively standardized in the literature and thus transformations there will be unwarranted (Wang et al., 2022; Azad et al., 2023). In comparison, as we mention in Section 1, in the MTRL setting, rewards for different tasks might be designed on very different scales.

Metaworld MT10 (Yu et al., 2020b). This benchmark consists of a robot arm conducting 10 tasks in the MuJoCo simulator (Todorov et al., 2012), each with distinct reward functions. The list of the 10 tasks is given in Appendix E.

MTRL baselines and metrics. As all DiBS-MTL variants are transformation invariant, we restrict our study to 1-step DiBS-MTL, which has the lowest per epoch complexity. We compare 1-step DiBS-MTL with (1) LS, (2) UW, (3) FAMO, (4) Fairgrad (Ban & Ji, 2024), (5) Nash-MTL (Navon et al., 2022) and (6) CAGrad (Liu et al., 2021a). Following prior work, for every method, we use Soft Actor-Critic (SAC) (Haarnoja et al., 2018) as the underlying reinforcement learning algorithm, hyperparameters

¹We were unable to reproduce the baseline plots reported in the original FAMO paper (Liu et al., 2023). The results shown here were obtained by strictly following the default parameters and instructions in the publicly available FAMO repository <https://github.com/Cranial-XIX/FAMO>.

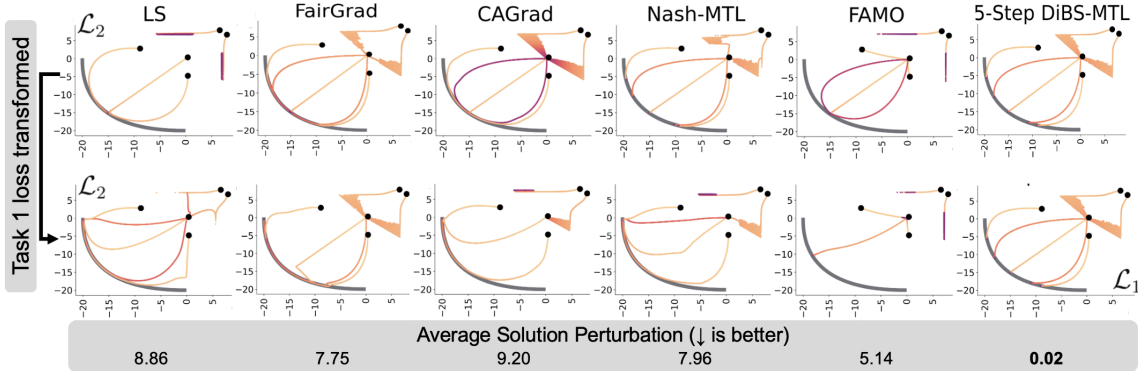


Figure 2. DiBS-MTL successfully avoids task domination due to its invariance to monotonic nonaffine transformations, while baseline MTL methods visibly favor task 1 when \mathcal{L}_1 is transformed, and some baseline methods even fail to reach the Pareto front. \bullet and — denote initializations and the Pareto front respectively. To better visualize results for the transformed case, we retain the original \mathcal{L}_1 axis. Results for multi-step DiBS-MTL and additional baselines are included in Figure 5.

Table 1. 1-step DiBS-MTL achieves robustness to the different reward transformations on the MT10 multi-task reinforcement learning benchmark, and significantly outperforms all MTL baselines for all transformed settings. We report best-checkpoint success (evaluated every 200 episodes) mean results \pm standard error over 10 seeds. **Bold** values indicate best performances per column. \dagger For certain transformations, training with UW, Nash-MTL, FairGrad, and CAGrad was highly sensitive to loss scaling. This instability caused the training process to diverge, leading the underlying MuJoCo simulator (Todorov et al., 2012) to repeatedly produce out-of-bounds errors. As a result, we were unable to collect results for these cases.

	Transformed task			
	No task transformed	reach transformed	window open transformed	peg insert transformed
FAMO	0.920 \pm 0.020	0.700 \pm 0.075	0.830 \pm 0.033	0.570 \pm 0.070
LS	0.850 \pm 0.040	0.480 \pm 0.044	0.200 \pm 0.026	0.230 \pm 0.030
UW	0.830 \pm 0.033	0.650 \pm 0.081	— \dagger	0.420 \pm 0.074
FairGrad	0.950 \pm 0.022	0.290 \pm 0.023	— \dagger	— \dagger
Nash-MTL	0.970 \pm 0.015	— \dagger	— \dagger	— \dagger
CAGrad	0.950 \pm 0.022	0.689 \pm 0.031	— \dagger	— \dagger
1-step DiBS-MTL	0.890 \pm 0.023	0.850 \pm 0.022	0.920 \pm 0.025	0.700 \pm 0.037

values are taken from the corresponding baseline works, and we report the fraction of tasks successfully completed (Navon et al., 2022; Liu et al., 2023), where the definition of task success is as described in the Meta-World benchmark (Yu et al., 2020b). Reported results have been averaged over 10 random seeds. Complete implementation details and hyperparameter values are in Appendix E.

Task transformations in the MTRL setup. We consider transformation of 3 different tasks—for each, we apply monotonic, nonaffine transformations to the underlying reward function. For actor-critic algorithms like SAC, this transformation corresponds to potentially nonmonotonic, nonaffine critic loss transformations. This is because the losses fit the collected rewards to value functions rather than fitting the state dependent rewards. Thus, these task reward transformations can lead to potentially *nonmonotonic* task loss transformations. However, we remark that in the policy landscape, a good policy for the nominal reward is also

likely to perform well for the transformed reward.

Reward transformations. We consider the following task-transformation pairs: (i) $h(r) = \text{sign}(r) \cdot r^4$ for reach, (ii) $h(r) = (5 + r)^4$ for peg insert, (h is monotonic over the reward range), and (iii) $h(r) = \exp(r)$ for window open. These transformations were arbitrarily selected to illustrate a range of functional forms and tasks.

DiBS-MTL displays robustness against nonaffine reward transformations, while baselines drastically degrade. Figures 3a to 3d and Table 1 show that 1-step DiBS-MTL achieves remarkable robustness to the different reward transformations compared to existing MTL methods. While gradient-based MTL methods like FairGrad, Nash-MTL and CAGrad display strong performance in the nominal setting, their performance significantly degrades in the transformed cases, often to the extent that training became unstable, and the underlying MuJoCo simulator

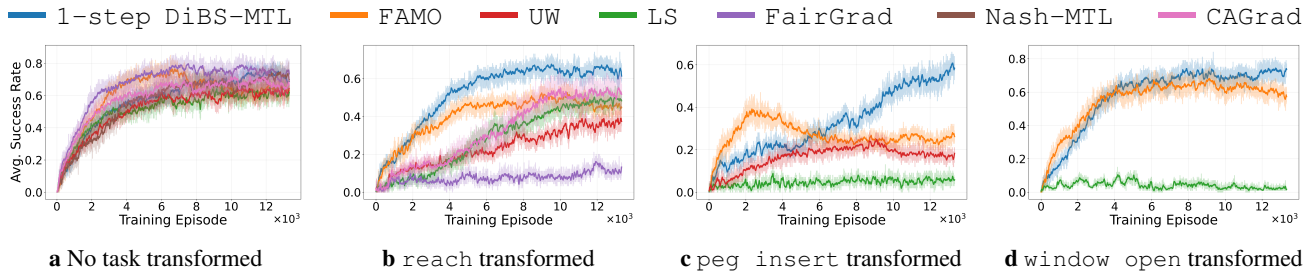


Figure 3. Average task success rate on the MT10 benchmark, averaged over all tasks and 10 random seeds. Transparent curves show per-episode success rates, while solid curves denote rolling averages computed over a window of 51 episodes. 1-step DiBS-MTL demonstrates strong robustness to diverse reward transformations and consistently and significantly outperforms all baselines across all transformed settings.

(Todorov et al., 2012) consistently gave out of bound errors for many seeds. Out of all methods, 1-step DiBS-MTL achieves state-of-the-art overall robustness for all transformed cases, while other methods either fail or exhibit significant performance drops for all transformations compared to their performance in the nominal setting. Finally, DiBS-MTL again achieves faster runtimes than the previous bargaining-inspired MTL method Nash-MTL (see Section F.1).

Takeaway from Sections 5.1 and 5.2:

DiBS-MTL significantly outperforms state-of-the-art MTL baselines in all examples where underlying task losses/rewards are poorly scaled relative to each other, thanks to its monotonic transformation invariance. This highlights the unique suitability of DiBS-MTL to MTL problems with heterogeneous, possibly unknown task loss scalings.

5.3. Can the transformation robust DiBS-MTL maintain competitive performance in untransformed settings on standard MTL benchmarks?

To compare DiBS-MTL with existing methods in large-scale learning examples, we perform experiments in supervised learning in two domains—(i) computer vision (the NYU-v2 dataset (Silberman et al., 2012)), and (ii) graph neural networks for quantum chemistry (QM9 dataset (Blum & Raymond, 2009)). Additional results for the computer vision Cityscapes dataset (Cordts et al., 2016) are included in Section D. All of these are widely used challenging benchmarks in MTL literature (Liu et al., 2021a; Navon et al., 2022; Liu et al., 2023; Xiao et al., 2025; Dai et al., 2023; Shen et al., 2024; Ban & Ji, 2024), and complete benchmark descriptions are given in Section E. We begin by describing the baselines and metrics for all datasets. We keep the default training procedures established in prior baseline works for a fair comparison. All implementation details are given in Appendix E.

Supervised MTL baselines. For all datasets, we compare 1-Step, 5-Step, and 10-Step DiBS-MTL with an extensive suite of strong MTL baselines: (1) linear scalarization (LS), (2) uncertainty weighting (UW) (Kendall et al., 2018), (3) MGDA (Sener & Koltun, 2018), (4) Nash-MTL (Navon et al., 2022), (5) FAMO (Liu et al., 2023), (6) GO4Align (Shen et al., 2024), (7) IGBv2, (8) IGBv2+Nash (Dai et al., 2023), and (9) LDC (Xiao et al., 2025). For all baselines across all datasets, the architecture, data pipeline, protocols, and training hyperparameters are taken to be the same as that in the corresponding works introducing the baselines.

Supervised MTL metrics. In addition to task-specific metrics, we evaluate all methods using two standard measures of multi-task performance: (1) the mean relative per-task performance drop $\Delta m\%$ with respect to single-task learning (STL), and (2) the mean rank (MR) across all task metrics. $\Delta m\%$ captures the average improvement or degradation relative to independent single task training (STL), while MR summarizes the average rank of a method across all tasks for a benchmark. These metrics are used in all baseline works as well, to assess whether an MTL method improves joint learning across diverse tasks.

DiBS-MTL achieves competitive performance across all datasets. Table 2 reports results on NYU-v2. DiBS-MTL variants achieve state-of-the-art performance in $\Delta m\%$ as well as MR, being the best or second-best in both MTL relevant metrics across all methods, demonstrating balanced improvements across segmentation, depth, and normal prediction. DiBS-MTL variants also achieve competitive or superior performance in segmentation and depth estimation, while matching strong baselines on surface normal prediction. In the QM9 benchmark, DiBS-MTL variants display superior performance for the α and c_v prediction tasks. Additionally, DiBS-MTL variants achieve the best $\Delta m\%$ and second best MR performance (Table 3). Finally, 1-step DiBS-MTL is faster than Nash-MTL for NYU-v2, and only slightly slower on QM9 (Section F.1).

Table 2. DiBS-MTL variants exhibit strong performance on the NYU-v2 benchmark, achieving state of the art values on MTL relevant metrics ($\Delta m\%$ & MR). **Bold/underline** indicates best/second-best performance per column. Results averaged over 3 random seeds.

	Segmentation		Depth Estimation		Surface Normal					$\Delta m\% \downarrow$	MR \downarrow
	mIoU \uparrow	Pix Acc \uparrow	Abs Err \downarrow	Rel Err \downarrow	Median \downarrow	Mean \downarrow	$< 30 \uparrow$	$< 22.5 \uparrow$	$< 11.25 \uparrow$		
STL	38.30	63.76	0.68	0.28	19.21	25.01	69.15	57.20	30.14	—	—
MGDA	32.03	60.77	0.6102	0.2453	19.00	24.64	69.83	57.78	30.55	-0.69	11.0
UW	39.08	64.73	0.5464	0.2284	23.04	27.34	62.85	49.23	23.49	3.77	8.2
Nash-MTL	40.16	65.65	<u>0.5331</u>	0.2203	19.96	25.25	68.29	55.72	28.62	-3.98	4.2
FAMO	37.58	64.08	0.5595	0.2296	<u>19.15</u>	<u>25.04</u>	<u>69.36</u>	<u>57.44</u>	<u>30.23</u>	-3.82	8.5
LS	40.16	65.63	0.5445	0.2223	23.03	27.50	62.66	49.32	23.61	3.06	6.0
GO4Align	38.87	64.52	0.5698	0.2406	23.41	27.81	61.83	48.56	23.45	5.47	9.9
IGBV2	33.61	61.88	0.5728	0.2222	23.18	27.94	62.14	49.10	23.59	11.92	9.7
IGBV2+Nash	38.81	65.66	0.5258	0.2086	20.09	25.50	67.82	55.35	28.37	1.67	5.1
LDC	39.21	65.70	0.5337	<u>0.2180</u>	20.23	25.29	67.98	55.19	27.98	-3.24	4.5
1-step DiBS-MTL	40.92	66.60	0.5337	0.2216	20.06	25.35	68.15	55.54	28.54	-4.11	3.1
5-step DiBS-MTL	<u>41.27</u>	67.10	0.5473	0.2300	19.69	25.13	68.69	56.28	29.31	<u>-4.57</u>	4.2
10-step DiBS-MTL	41.33	<u>67.09</u>	0.5381	0.2260	19.77	25.06	68.67	56.12	29.02	-4.74	<u>3.6</u>

Table 3. DiBS-MTL exhibits strong performance on the QM9 benchmark, with the 10-step variant achieving best and second-best values on MTL relevant metrics $\Delta m\%$ & MR. **Bold/underline** indicates best/second-best performance. Results averaged over 3 random seeds.

	μ	α	ϵ_{HOMO}	ϵ_{LUMO}	$\langle R^2 \rangle$	ZPVE	U_0	U	H	G	c_v	$\Delta m\% \downarrow$	MR \downarrow
	MAE \downarrow												
STL	0.07	0.18	60.60	53.90	0.50	4.53	58.80	64.20	63.80	66.20	0.07	—	—
LS	0.0998	0.3108	69.83	84.87	5.13	13.43	137.25	137.97	138.43	133.55	0.1226	167.16	7.42
GO4ALIGN	0.1047	0.3175	<u>70.40</u>	86.48	5.05	13.35	138.78	139.49	139.86	135.27	0.1252	167.90	7.88
UW	0.4123	0.3937	159.07	145.41	1.09	4.85	<u>61.52</u>	<u>61.95</u>	<u>61.98</u>	<u>61.40</u>	0.1206	102.96	5.50
LDC	0.2782	0.3318	141.53	121.37	1.20	4.34	51.43	51.83	51.91	51.28	0.1076	<u>68.79</u>	3.50
FAMO	0.4422	0.3998	158.41	145.83	<u>1.10</u>	5.04	65.76	66.15	66.24	65.40	0.1267	110.99	6.67
Nash-MTL	<u>0.1024</u>	0.3153	70.75	<u>85.29</u>	5.05	13.04	135.67	136.55	136.82	132.71	0.1227	165.12	6.96
IGBV2	0.2866	0.3557	149.29	135.04	1.24	<u>4.60</u>	64.68	65.08	65.15	64.92	0.1176	85.75	5.33
IGBV2 + Nash	0.4399	0.3762	142.19	139.73	1.62	5.10	67.20	67.61	67.66	67.13	0.1159	115.24	7.17
1-step DiBS-MTL	0.1347	0.2841	97.53	95.01	2.56	5.75	65.92	66.38	66.39	65.83	0.1067	71.83	<u>4.83</u>
5-step DiBS-MTL	0.1285	0.2914	96.40	95.95	2.55	5.68	69.28	69.68	69.74	69.11	<u>0.1065</u>	72.92	5.54
10-step DiBS-MTL	0.1213	<u>0.2860</u>	93.50	90.46	2.37	5.81	70.12	70.54	70.75	69.83	0.1061	67.37	5.21

Takeaway from Section 5.3:

Across all large-scale untransformed benchmark evaluations, DiBS-MTL consistently performs competitively against leading MTL baselines. This indicates that the transformation robustness property of DiBS-MTL does not sacrifice performance on popular real-world benchmarks.

6. Conclusion

We consider the problem of constructing multi-task learning (MTL) methods that are robust to monotonic, nonaffine task loss transformations. In practice, different task losses can be arbitrarily scaled with respect to one another, and those scalings can be understood as monotonic, possibly nonaffine transformations of some ideal, unknown losses which are meaningfully comparable. To address this problem, we present DiBS-MTL, an MTL method which is invariant to such transformations because it uses only normalized task

loss gradients. Building upon recent work which formalizes the MTL training update step as a bargaining game played between tasks (Navon et al., 2022), we adapt the recently introduced DiBS bargaining approach (Gupta et al., 2025) in order to find a Pareto stationary (and monotonic transformation-invariant) update direction. While DiBS enjoys convergence guarantees when losses are strongly convex, practical MTL problems almost always have nonconvex task losses. To bridge this gap, we prove that a subsequence of the DiBS iterates asymptotically converges to a Pareto stationary point even in the nonconvex regime. Empirically, we demonstrate that (i) due to its monotonic transformation invariance, DiBS-MTL significantly outperforms state-of-the-art MTL baselines in settings with task losses being poorly scaled relative to each other, highlighting the unique suitability of DiBS-MTL to MTL problems with heterogeneous, possibly unknown task loss scalings; and (ii) the transformation robustness property of DiBS-MTL does not sacrifice performance on real-world benchmarks, where DiBS-MTL is competitive against leading MTL baselines.

Impact Statement

This paper presents work whose goal is to advance the field of Machine Learning. There are many potential societal consequences of our work, none which we feel must be specifically highlighted here.

Acknowledgments

This work was supported by the Air Force Office for Scientific Research under grant number FA9550-22-1-0403, Lockheed Martin under number MRA16-005-RPP023, DARPA Transfer from Imprecise and Abstract Models to Autonomous Technologies (TIAMAT) under grant number HR0011-24-9-0431, the National Science Foundation under awards 2336840 and 2211548, and by the Army Research Laboratory under Cooperative Agreement Number W911NF-25-2-0021.

References

- Azad, R., Heidary, M., Yilmaz, K., Hüttemann, M., Karim-ijafarbigloo, S., Wu, Y., Schmeink, A., and Merhof, D. Loss functions in the era of semantic segmentation: A survey and outlook. *arXiv preprint arXiv:2312.05391*, 2023.
- Badrinarayanan, V., Kendall, A., and Cipolla, R. Segnet: A deep convolutional encoder-decoder architecture for image segmentation. *IEEE transactions on pattern analysis and machine intelligence*, 39(12):2481–2495, 2017.
- Ban, H. and Ji, K. Fair resource allocation in multi-task learning. In *International Conference on Machine Learning*, pp. 2715–2731. PMLR, 2024.
- Blum, L. C. and Reymond, J.-L. 970 million druglike small molecules for virtual screening in the chemical universe database gdb-13. *Journal of the American Chemical Society*, 131(25):8732–8733, 2009.
- Chen, Z., Badrinarayanan, V., Lee, C.-Y., and Rabinovich, A. Gradnorm: Gradient normalization for adaptive loss balancing in deep multitask networks. In *International conference on machine learning*, pp. 794–803. PMLR, 2018.
- Chen, Z., Ngiam, J., Huang, Y., Luong, T., Kretzschmar, H., Chai, Y., and Anguelov, D. Just pick a sign: Optimizing deep multitask models with gradient sign dropout. *Advances in Neural Information Processing Systems*, 33: 2039–2050, 2020.
- Cordts, M., Omran, M., Ramos, S., Rehfeld, T., Enzweiler, M., Benenson, R., Franke, U., Roth, S., and Schiele, B. The cityscapes dataset for semantic urban scene understanding. In *Proceedings of the IEEE conference on computer vision and pattern recognition*, pp. 3213–3223, 2016.
- Dai, Y., Fei, N., and Lu, Z. Improvable gap balancing for multi-task learning. In *Uncertainty in Artificial Intelligence*, pp. 496–506. PMLR, 2023.
- Désidéri, J.-A. Multiple-gradient descent algorithm (mgda) for multiobjective optimization. *Comptes Rendus Mathématique*, 350(5-6):313–318, 2012.
- Fey, M. and Lenssen, J. E. Fast graph representation learning with pytorch geometric. *arXiv preprint arXiv:1903.02428*, 2019.
- Fifty, C., Amid, E., Zhao, Z., Yu, T., Anil, R., and Finn, C. Efficiently identifying task groupings for multi-task learning. *Advances in Neural Information Processing Systems*, 34:27503–27516, 2021.
- Gao, Y., Bai, H., Jie, Z., Ma, J., Jia, K., and Liu, W. Mtl-nas: Task-agnostic neural architecture search towards general-purpose multi-task learning. In *Proceedings of the IEEE/CVF Conference on computer vision and pattern recognition*, pp. 11543–11552, 2020.
- Gilmer, J., Schoenholz, S. S., Riley, P. F., Vinyals, O., and Dahl, G. E. Neural message passing for quantum chemistry. In *International conference on machine learning*, pp. 1263–1272. Pmlr, 2017.
- Goodfellow, I. J., Vinyals, O., and Saxe, A. M. Qualitatively characterizing neural network optimization problems. *arXiv preprint arXiv:1412.6544*, 2014.
- Guo, P., Lee, C.-Y., and Ulbricht, D. Learning to branch for multi-task learning. In *International conference on machine learning*, pp. 3854–3863. PMLR, 2020.
- Gupta, K., Murthy, S., Karabag, M. O., Topcu, U., and Fridovich-Keil, D. Cooperative bargaining games without utilities: Mediated solutions from direction oracles. In *The Thirty-ninth Annual Conference on Neural Information Processing Systems*, 2025. URL <https://openreview.net/forum?id=DcpUkPHRJw>.
- Haarnoja, T., Zhou, A., Abbeel, P., and Levine, S. Soft actor-critic: Off-policy maximum entropy deep reinforcement learning with a stochastic actor. In *International conference on machine learning*, pp. 1861–1870. Pmlr, 2018.
- Hu, Y., Xian, R., Wu, Q., Fan, Q., Yin, L., and Zhao, H. Revisiting scalarization in multi-task learning: A theoretical perspective. *Advances in Neural Information Processing Systems*, 36:48510–48533, 2023.

- Kendall, A., Gal, Y., and Cipolla, R. Multi-task learning using uncertainty to weigh losses for scene geometry and semantics. In *Proceedings of the IEEE conference on computer vision and pattern recognition*, pp. 7482–7491, 2018.
- Kingma, D. P. and Ba, J. Adam: A method for stochastic optimization. *CoRR*, abs/1412.6980, 2014.
- Kokkinos, I. Ubernet: Training a universal convolutional neural network for low-, mid-, and high-level vision using diverse datasets and limited memory. In *Proceedings of the IEEE conference on computer vision and pattern recognition*, pp. 6129–6138, 2017.
- Kurin, V., De Palma, A., Kostrikov, I., Whiteson, S., and Mudigonda, P. K. In defense of the unitary scalarization for deep multi-task learning. *Advances in Neural Information Processing Systems*, 35:12169–12183, 2022.
- Lin, B., Ye, F., Zhang, Y., and Tsang, I. Reasonable effectiveness of random weighting: A litmus test for multi-task learning. *Transactions on Machine Learning Research*, 2022. ISSN 2835-8856.
- Liu, B., Liu, X., Jin, X., Stone, P., and Liu, Q. Conflict-averse gradient descent for multi-task learning. *Advances in Neural Information Processing Systems*, 34:18878–18890, 2021a.
- Liu, B., Feng, Y., Stone, P., and Liu, Q. Famo: Fast adaptive multitask optimization. *Advances in Neural Information Processing Systems*, 36:57226–57243, 2023.
- Liu, L., Li, Y., Kuang, Z., Xue, J.-H., Chen, Y., Yang, W., Liao, Q., and Zhang, W. Towards impartial multi-task learning. In *International Conference on Learning Representations*, 2021b. URL <https://openreview.net/forum?id=IMPnRXEWpvr>.
- Liu, S., Johns, E., and Davison, A. J. End-to-end multi-task learning with attention. In *Proceedings of the IEEE/CVF conference on computer vision and pattern recognition*, pp. 1871–1880, 2019.
- Narahari, Y. *Game theory and mechanism design*, volume 4. World Scientific, 2014.
- Nash, J. F. et al. The bargaining problem. *Econometrica*, 18(2):155–162, 1950.
- Navon, A., Shamsian, A., Achituve, I., Maron, H., Kawaguchi, K., Chechik, G., and Fetaya, E. Multi-task learning as a bargaining game. In *International Conference on Machine Learning*, pp. 16428–16446. PMLR, 2022.
- Robbins, H. and Monro, S. A stochastic approximation method. *The annals of mathematical statistics*, pp. 400–407, 1951.
- Sener, O. and Koltun, V. Multi-task learning as multi-objective optimization. *Advances in neural information processing systems*, 31, 2018.
- Shen, J., Wang, Q., Xiao, Z., Van Noord, N., and Worring, M. Go4align: Group optimization for multi-task alignment. *Advances in Neural Information Processing Systems*, 37:111382–111405, 2024.
- Silberman, N., Hoiem, D., Kohli, P., and Fergus, R. Indoor segmentation and support inference from rgbd images. In *European conference on computer vision*, pp. 746–760. Springer, 2012.
- Sodhani, S. and Zhang, A. Mtrl - multi task rl algorithms. Github, 2021. URL <https://github.com/facebookresearch/mtrl>.
- Song, X., Zheng, S., Cao, W., Yu, J., and Bian, J. Efficient and effective multi-task grouping via meta learning on task combinations. *Advances in Neural Information Processing Systems*, 35:37647–37659, 2022.
- Standley, T., Zamir, A., Chen, D., Guibas, L., Malik, J., and Savarese, S. Which tasks should be learned together in multi-task learning? In *International conference on machine learning*, pp. 9120–9132. PMLR, 2020.
- Thomson, W. Cooperative models of bargaining. *Handbook of game theory with economic applications*, 2:1237–1284, 1994.
- Todorov, E., Erez, T., and Tassa, Y. Mujoco: A physics engine for model-based control. In *2012 IEEE/RSJ International Conference on Intelligent Robots and Systems*, pp. 5026–5033. IEEE, 2012. doi: 10.1109/IROS.2012.6386109.
- Vinyals, O., Bengio, S., and Kudlur, M. Order matters: Sequence to sequence for sets. *arXiv preprint arXiv:1511.06391*, 2015.
- Wang, Q., Ma, Y., Zhao, K., and Tian, Y. A comprehensive survey of loss functions in machine learning. *Annals of Data Science*, 9(2):187–212, 2022.
- Xiao, P., Dong, C., Zou, S., and Ji, K. Ldc-mtl: Balancing multi-task learning through scalable loss discrepancy control. *arXiv preprint arXiv:2502.08585*, 2025.
- Xin, D., Ghorbani, B., Gilmer, J., Garg, A., and Firat, O. Do current multi-task optimization methods in deep learning even help? *Advances in neural information processing systems*, 35:13597–13609, 2022.

Yu, R., Wan, S., Wang, Y., Gao, C.-X., Gan, L., Zhang, Z., and Zhan, D.-C. Reward models in deep reinforcement learning: A survey. *arXiv preprint arXiv:2506.15421*, 2025.

Yu, T., Kumar, S., Gupta, A., Levine, S., Hausman, K., and Finn, C. Gradient surgery for multi-task learning. *Advances in neural information processing systems*, 33: 5824–5836, 2020a.

Yu, T., Quillen, D., He, Z., Julian, R., Hausman, K., Finn, C., and Levine, S. Meta-world: A benchmark and evaluation for multi-task and meta reinforcement learning. In *Conference on robot learning*, pp. 1094–1100. PMLR, 2020b.

Contents

A Proof of Theorem 1	12
B Relaxing Assumption 2	14
C Discussion on IMTL-G	15
D Additional Supervised MTL Experiments – Cityscapes benchmark	15
E Experimental Details and Code base	16
E.1 Demonstrative Nonconvex Example	16
E.2 NYuV2	16
E.3 Cityscapes	16
E.4 QM9	17
E.5 Meta-World MT10	17
F Additional Results	18
F.1 Comparison of DiBS-MTL runtimes with previous bargaining MTL method Nash-MTL.	18
F.2 Additional Results in the Demonstrative Nonconvex Example	19
G 1-step DiBS-MTL Algorithm Pseudocode	20

A. Proof of Theorem 1

Proof sketch. As the iterates are bounded, there exists a subsequence which converges to some cluster point \mathbf{x}^\dagger . To show that \mathbf{x}^\dagger is a Pareto stationary point, we will show by contradiction that $h(\mathbf{x}^\dagger) = 0$.

Proof. Because the DiBS iterates $\{\mathbf{x}_k\}_{k=1}^\infty$ is a bounded sequence from Assumption 2 (relaxed in Section B), by Bolzano-Weierstrass theorem, $\exists \mathbf{x}^\dagger \in \mathcal{S}$ such that a subsequence of the sequence $\{\mathbf{x}_k\}_{k=1}^\infty$ converges to \mathbf{x}^\dagger , and that for every neighborhood \mathcal{U} of \mathbf{x}^\dagger , there exist infinite $n \in \mathbb{N}$ such that $\mathbf{x}_n \in \mathcal{U}$. We will show by contradiction that $h(\mathbf{x}^\dagger) = 0$. Let there exist an $a > 0$ such that $\|h(\mathbf{x}^\dagger)\|_2 = a$. We define

$$M := \sup_{\mathbf{x} \in \mathcal{D}} \|h(\mathbf{x})\|_2, \quad u := \frac{h(\mathbf{x}^\dagger)}{\|h(\mathbf{x}^\dagger)\|_2}$$

Then, by continuity of $u^\top h(\mathbf{x})$, we have

$$\forall \delta > 0, \exists \epsilon > 0 \text{ such that } \|\mathbf{x} - \mathbf{x}^\dagger\|_2 \leq \delta \implies u^\top h(\mathbf{x}) \geq a\epsilon, \quad (2)$$

$$\text{and } \exists N \in \mathbb{N} \text{ such that } k \geq N \implies \alpha_k \leq \frac{a}{C} \text{ for some } C > 0. \quad (3)$$

Let $\mathcal{V}(\mathbf{x}, r)$ denote a ball in \mathbb{R}^n centered at $\mathbf{x} \in \mathbb{R}^n$, with radius r . Let us pick a $\tilde{\delta} > 0$, and analyse the DiBS iterations when they are in $\mathcal{V}(\mathbf{x}^\dagger, \tilde{\delta})$. Because there are an infinite number of n such that $\mathbf{x}_n \in \mathcal{V}(\mathbf{x}^\dagger, \tilde{\delta})$, there are two possibilities:

- Case 1.** $\exists \delta > \tilde{\delta}$ such that the DiBS iterates enter $\mathcal{V}(\mathbf{x}^\dagger, \tilde{\delta})$, exit $\mathcal{V}(\mathbf{x}^\dagger, \delta)$, and then re-enter $\mathcal{V}(\mathbf{x}^\dagger, \tilde{\delta})$ —an infinite number of times.
- Case 2.** The DiBS iterates enter $\mathcal{V}(\mathbf{x}^\dagger, \tilde{\delta})$ and then exit it at most a finite number of times before eventually remaining in $\mathcal{V}(\mathbf{x}^\dagger, \tilde{\delta})$ forever.

Case 1. Consider the counts when the DiBS iterates are inside $\mathcal{V}(\mathbf{x}^\dagger, \tilde{\delta})$, $n < t_1 < t_2 < \dots$ such that $\mathbf{x}_{t_k} \in \mathcal{V}(\mathbf{x}^\dagger, \tilde{\delta}) \forall k \in \mathbb{N}$, and let the earliest corresponding counts when the DiBS iterates are outside $\mathcal{V}(\mathbf{x}^\dagger, \delta)$ be $e_k := \min\{t \geq t_k | \mathbf{x}_t \notin \mathcal{V}(\mathbf{x}^\dagger, \delta)\}$. Then, from Equation (2), we have

$$u^\top h(\mathbf{x}_t) \geq a\epsilon \forall t = t_k, t_{k+1}, \dots, e_k - 1.$$

Now, from the definition of t_k and e_k , we have

$$\begin{aligned} & \|\mathbf{x}_{e_k} - \mathbf{x}_{t_k}\|_2 \geq \delta - \tilde{\delta} > 0 \\ \implies & \left\| \sum_{t=t_k}^{e_k-1} (\mathbf{x}_{t+1} - \mathbf{x}_t) \right\|_2 \geq \delta - \tilde{\delta} \\ \implies & \sum_{t=t_k}^{e_k-1} \|\mathbf{x}_{t+1} - \mathbf{x}_t\|_2 \geq \delta - \tilde{\delta} \quad (\text{triangle inequality}) \\ \implies & \sum_{t=t_k}^{e_k-1} \alpha_t = \sum_{t=t_k}^{e_k-1} \frac{\|\mathbf{x}_{t+1} - \mathbf{x}_t\|_2}{\|h(\mathbf{x}_t)\|_2} \geq \sum_{t=t_k}^{e_k-1} \frac{\|\mathbf{x}_{t+1} - \mathbf{x}_t\|_2}{M} \geq \frac{(\delta - \tilde{\delta})}{M} \\ \implies & u^\top (\mathbf{x}_{e_k} - \mathbf{x}_{t_k}) = \sum_{t=t_k}^{e_k-1} u^\top (\mathbf{x}_{t+1} - \mathbf{x}_t) = - \sum_{t=t_k}^{e_k-1} \alpha_t u^\top h(\mathbf{x}_t) \\ & \leq -a\epsilon \sum_{t=t_k}^{e_k-1} \alpha_t \quad (\text{from Equation (2)}) \\ \implies & u^\top (\mathbf{x}_{e_k} - \mathbf{x}_{t_k}) \leq -\frac{a\epsilon (\delta - \tilde{\delta})}{M}. \quad (4) \end{aligned}$$

Here, the first equality could be legitimately written as the definition of case 1 implies that $h(\mathbf{x}_t) \neq 0, t = t_k, \dots, e_k - 1$, otherwise the iterates would have remained within $\mathcal{V}(\mathbf{x}^\dagger, \tilde{\delta})$ forever. Now, from the definition of case 1, t_{k+1} and e_k , we have that the DiBS iterates cannot remain outside $\mathcal{V}(\mathbf{x}^\dagger, \tilde{\delta})$ for an infinite amount of time, and thus $\exists C' > 0$ such that $C' > \sum_{t=e_k}^{t_{k+1}-1} 1 \forall k$. Thus

$$\begin{aligned} u^\top (\mathbf{x}_{t_{k+1}} - \mathbf{x}_{e_k}) &= \sum_{t=e_k}^{t_{k+1}-1} u^\top (\mathbf{x}_{t+1} - \mathbf{x}_t) \\ &\leq \sum_{t=e_k}^{t_{k+1}-1} \alpha_t M \quad (\text{Cauchy-Schwarz}) \\ &= M \sum_{t=e_k}^{t_{k+1}-1} \alpha_t \\ &\leq \frac{aMC'}{C} \quad (\text{from Equation (3)}) \\ \implies u^\top (\mathbf{x}_{t_{k+1}} - \mathbf{x}_{e_k}) &\leq \frac{aMC'}{C} := a\gamma. \quad (5) \end{aligned}$$

Combining Equations (4) and (5), we get

$$\begin{aligned} u^\top (\mathbf{x}_{t_{k+1}} - \mathbf{x}_{t_k}) &\leq a \left(\gamma - \frac{\epsilon (\tilde{\delta} - \delta)}{M} \right) \\ \implies u^\top \mathbf{x}_{t_{k+1}} &\leq u^\top \mathbf{x}_{t_1} + k \cdot a \left(\gamma - \frac{\epsilon (\tilde{\delta} - \delta)}{M} \right) \quad (6) \end{aligned}$$

From Cauchy-Schwarz inequality, $\|u^\top \mathbf{x}_{t_{k+1}}\|_2 \leq \|\mathbf{x}_{t_{k+1}}\|_2$ is bounded for all $k \in \mathbb{N}$ as the DiBS sequence is bounded. However, from Equation (6), as k increases $\|u^\top \mathbf{x}_{t_{k+1}}\|_2$ becomes unbounded, which is a **contradiction**.

Case 2. By definition of case 2, $\exists t^* < \infty$ such that $\mathbf{x}_t \in \mathcal{V}(\mathbf{x}^\dagger, \delta) \forall t \geq t^*$. Thus for $T > t^*$, we have

$$\begin{aligned}
 u^\top (\mathbf{x}_T - \mathbf{x}_{t^*}) &= \sum_{t=t^*}^{T-1} u^\top (\mathbf{x}_{t+1} - \mathbf{x}_t) \\
 &= - \sum_{t=t^*}^{T-1} \alpha_t u^\top h(\mathbf{x}_t) \\
 &\leq -a\epsilon \sum_{t=t^*}^{T-1} \alpha_t \quad (\text{from Equation (2)}) \\
 \implies u^\top \mathbf{x}_T &\leq u^\top \mathbf{x}_{t^*} - a\epsilon \sum_{t=t^*}^{T-1} \alpha_t \quad (7)
 \end{aligned}$$

Similar to the argument of contradiction in case 1, $\|u^\top \mathbf{x}_{t^*}\|_2, \|u^\top \mathbf{x}_T\|_2, T \geq t^*$ are bounded. However, Equation (7) suggests that $\|u^\top \mathbf{x}_T\|$ becomes unbounded as T increases, because of the Robbins-Monro stepsize condition $\sum_k \alpha_k = \infty$, and $\sum_{k=1}^{t^*-1} \alpha_k$ is finite. Hence, we arrive at a **contradiction**.

Thus, from both cases, we get that $h(\mathbf{x}^\dagger) = 0$, and from Definition 1, \mathbf{x}^\dagger is a Pareto stationary point with convex coefficients

$$\beta^i = \frac{\|\mathbf{x}^\dagger - \mathbf{x}^{*,i}\|_2 / \|\nabla_{\mathbf{x}} \ell^i(\mathbf{x}^\dagger)\|_2}{\sum_i \|\mathbf{x}^\dagger - \mathbf{x}^{*,i}\|_2 / \|\nabla_{\mathbf{x}} \ell^i(\mathbf{x}^\dagger)\|_2}.$$

□

B. Relaxing Assumption 2

In the case when all agent (task) losses ℓ^i are convex, it has been established that the DiBS iterates are bounded (Gupta et al., 2025). In the non-convex setting, while the boundedness of the DiBS iterates intuitively holds for a problem with gradient conflict, i.e., task loss gradients point in opposite directions, we show that boundedness can be formally guaranteed with standard concepts from dynamical systems theory.

In particular, the following simple modification to DiBS allows us to guarantee boundedness, without changing the fact that the only fixed points of the dynamics are Pareto stationary points.

$$\mathbf{x}_{k+1} = \begin{cases} f_1(\mathbf{x}_k) := \mathbf{x}_k - h(\mathbf{x}_k), & \text{if } \|\mathbf{x}_k\|_2 \leq R \text{ (standard DiBS)} \\ f_2(\mathbf{x}_k) := \mathbf{x}_k - \alpha \frac{\mathbf{x}_k}{\|\mathbf{x}_k\|_2}, & \text{if } \|\mathbf{x}_k\|_2 \geq R + r \text{ (radially attractive)} \\ f(\mathbf{x}_k, t_k), & \text{if } R < \|\mathbf{x}_k\|_2 < R + r \text{ (convex combination)} \end{cases}$$

where $f(\mathbf{x}_k) = (1 - g(\mathbf{x}_k)) f_1(\mathbf{x}_k) + g(\mathbf{x}_k) f_2(\mathbf{x}_k) + z(\mathbf{x}_k, t_k)$,

$$z(\mathbf{x}_k, t_k) = \left(\frac{\|\mathbf{x}_k\|_2 - R}{r} \right) \cdot \left(1 - \frac{\|\mathbf{x}_k\|_2 - R}{r} \right) \cdot \sin(t) \mathbf{a}$$

$$g(\mathbf{x}) = \frac{e^{-\frac{r}{\|\mathbf{x}\|_2 - R}}}{e^{-\frac{r}{\|\mathbf{x}\|_2 - R}} + e^{-\frac{1}{1 - \frac{\|\mathbf{x}\|_2 - R}{r}}}}, \text{ and } t_k = \sum_{i=1}^k \mathbb{1}\{R < \|\mathbf{x}_i\|_2 < R + r\}$$

Here, $\mathbf{a} \in \mathbb{R}^n$ is any constant vector of the same dimension as the iterates \mathbf{x}_k . The radius R can be taken to be some large positive number, larger than $\max_i \|\mathbf{x}^{*,i}\|_2$, and r can be any positive constant. This modification ensures that (i) near the Pareto front, the DiBS iterates act as usual, (ii) in case the optimization landscape is such that due to a lack of conflicting gradient nature, the iterates somehow move away from the Pareto region and outside the $\|\mathbf{x}\|_2 \leq R + r$ ball, the iterates switch to the radially attractive dynamics and return to the ball and remain bounded, (iii) the dynamics switch is smoothly carried out in between the $\|\mathbf{x}\|_2 \leq R$ and $\|\mathbf{x}\|_2 \leq R + r$ balls, and (iv) the fixed points of the dynamics do not change—the time varying term $z(\mathbf{x}_k, t_k)$ ensures that only Pareto stationary points (all inside the $\|\mathbf{x}\|_R$ ball) are the fixed points of the modified dynamics, and the dynamics do not converge to non-Pareto stationary points.

Table 4. Results for supervised learning Cityscapes benchmark. Segmentation metrics (mIoU, Pix Acc) are shown in percentage form. **Bold**, underlined indicate best and second-best per column.

	Segmentation (%)		Depth Estimation			
	mIoU \uparrow	Pix Acc \uparrow	Abs Err \downarrow	Rel Err \downarrow	$\Delta m\%$ \downarrow	MR \downarrow
STL	74.01	93.16	0.0125	27.77	—	—
MGDA	69.44	91.49	0.0137	45.26	20.03	6.3
UW	66.18	90.28	0.0158	54.92	34.41	10.2
Nash-MTL	73.57	92.92	0.0140	52.34	25.30	6.0
FAMO	69.80	91.66	0.0137	<u>43.66</u>	<u>18.51</u>	5.5
LS	71.89	92.44	0.0180	111.89	87.64	10.0
GO4ALIGN	72.38	92.60	0.0312	93.50	97.26	9.8
IGBV2	66.44	90.48	0.0153	56.56	34.85	10.0
IGBV2+Nash	73.53	92.95	0.0135	50.42	22.58	4.5
LDC	75.04	<u>93.44</u>	0.0144	38.44	12.93	3.0
DiBS-MTL	74.64	93.31	0.0135	58.09	29.10	5.9
DiBS-MTL (5 Steps)	75.46	93.55	0.0132	54.88	25.27	<u>3.2</u>
DiBS-MTL (10 Steps)	<u>75.05</u>	93.41	<u>0.0133</u>	52.36	23.34	3.6

C. Discussion on IMTL-G

We elaborate on our claim made in Section 2 that though IMTL-G (Liu et al., 2021b) can be invariant to monotonic nonaffine transformations, it can produce Pareto solutions that are heavily favor one task over the other, possibly leading to task domination issues.

IMTL-G is a gradient-based method, which tries to find an update direction which has an equal projection on all task gradient vectors. Though this equal projection property brings invariance to monotonic nonaffine transformations, it also renders IMTL-G susceptible to task domination, as illustrated by the following simple two dimensional example.

Let $\mathcal{S} = [-1, 1] \times [-1, 1]$, with two tasks $\ell^1(x, y) = x^2 + (y - 1)^2$ and $\ell^2(x, y) = x^2 + (y + 1)^2$. Then any point of the form $(0, y), y \in [-1, 1]$ is a valid solution that IMTL-G can give. Even though all such points are Pareto stationary solutions, only $(0, 0)$ is balanced in the sense that it is equidistant to these symmetric functions (one function is a reflection of the other with respect to the X-axis). Thus IMTL-G can output a point like $(0, 0.9)$ which is heavily biased towards task 1. In contrast, even if the iterations are started at $(0, 0.9)$, DiBS will return the balanced point $(0, 0)$ as a solution.

D. Additional Supervised MTL Experiments – Cityscapes benchmark

The Cityscapes dataset (Cordts et al., 2016) contains 5000 street-view 128×256 , RGB images annotated for two tasks: (1) semantic segmentation with 19 classes and (2) discretized depth estimation with 7 ordinal bins. Following prior MTL evaluations on Cityscapes (Navon et al., 2022; Liu et al., 2023), we report mIoU and pixel accuracy for segmentation, and absolute and relative depth error for the depth task. This dataset complements NYU-v2 by providing a larger-scale, outdoor benchmark with visually and semantically different task relationships.

Results on Cityscapes. In the Cityscapes benchmark, DiBS-MTL variants similarly perform competitively against all baselines, achieving strong segmentation performance and favorable depth metrics across the two tasks (see Table 4), and the 5 step variant of DiBS-MTL achieves the second best MR.

E. Experimental Details and Code base

E.1. Demonstrative Nonconvex Example

Loss Functions. The non-convex objectives used in $(\mathcal{L}_1, \mathcal{L}_2)$ are given by

$$\begin{aligned} \mathcal{L}_1(\theta) &= c_1(\theta)f_1(\theta) + c_2(\theta)g_1(\theta), & \mathcal{L}_2(\theta) &= c_1(\theta)f_2(\theta) + c_2(\theta)g_2(\theta) \\ c_1(\theta) &= \max(\tanh(0.5\theta_2), 0), & c_2(\theta) &= \max(\tanh(-0.5\theta_2), 0), \\ f_1(\theta) &= \log\left(\max(|0.5(-\theta_1 - 7) - \tanh(-\theta_2)|, 10^{-6})\right) + 6, \\ f_2(\theta) &= \log\left(\max(|0.5(-\theta_1 + 3) - \tanh(-\theta_2) + 2|, 10^{-6})\right) + 6, \\ g_1(\theta) &= \frac{(-\theta_1 + 7)^2 + 0.1(-\theta_2 - 8)^2}{10} - 20, & g_2(\theta) &= \frac{(-\theta_1 - 7)^2 + 0.1(-\theta_2 - 8)^2}{10} - 20. \end{aligned}$$

As mentioned in Section 5, the transformation used on \mathcal{L}_1 for the transformed case is the monotonic, nonaffine transformation $h(\ell) = \text{sign}(\ell) \cdot \ell^4$.

E.2. NYUv2

Benchmark and Setup. The NYU-v2 indoor scene dataset (Silberman et al., 2012) provides 1,449 RGB-D images with dense per-pixel annotations for three tasks: semantic segmentation (13 classes), depth estimation, and surface normal prediction. Training uses standard task losses: per-pixel cross-entropy for segmentation, masked L1 for depth estimation over valid pixels, and a masked cosine loss over valid pixels for surface normal prediction. These choices match the NYU-v2 multi-task protocol followed by prior multi-task learning work (Liu et al., 2023; Navon et al., 2022). Our implementation builds on the official Nash-MTL code base² and incorporates the FAMO implementation³. Following standard practice (Liu et al., 2019; Navon et al., 2022; Liu et al., 2023; Xiao et al., 2025; Shen et al., 2024; Dai et al., 2023), we evaluate segmentation using mean Intersection-over-Union (mIoU) and pixel accuracy; depth estimation using mean absolute error and mean relative error; and surface normals using median angular error, mean angular error, and the percentage of pixels whose angular error is below 30° , 22.5° , and 11.25° (Silberman et al., 2012). These metrics provide a comprehensive view of per-task performance across classification, regression, and geometric prediction settings.

Model. The model architecture used in our experiments is a Multi-Task Attention Network (MTAN) (Liu et al., 2019) built on top of SegNet (Badrinarayanan et al., 2017). The network takes an RGB image as input and produces three task-specific outputs via separate heads: (i) a per-pixel class-score map for semantic segmentation, (ii) a scalar depth map for depth estimation, and (iii) a 3-channel surface-normal map for surface-normal prediction. For LS, MGDA, UW, FAMO, NashMTL, IGBv2, and DiBS-MTL, we use the multi-task attention network (MTAN) (Liu et al., 2019) with a SegNet-style encoder-decoder architecture and apply the same training schedule, optimizer, and data-augmentation procedures as established in prior work for a fair comparison. For LDC (Xiao et al., 2025) and GO4Align (Shen et al., 2024), we use the task architectures provided in their original implementations.

Training Protocol. For training, we follow the procedure outlined in (Navon et al., 2022). We train for 200 epochs with Adam (Kingma & Ba, 2014), using an initial learning rate of 1×10^{-4} reduced to 5×10^{-5} after 100 epochs. All reported results are averaged over three random seeds, namely 1, 7, and 42.

E.3. Cityscapes

Benchmark and Setup. The Cityscapes outdoor driving scenes (Cordts et al., 2016) provides 5000 RGB-D images with dense per-pixel annotations for 2 tasks: semantic segmentation (7 classes) and depth estimation. Training uses standard task losses: per-pixel cross-entropy for segmentation and masked L1 for depth estimation over valid pixels. These choices match the Cityscapes multi-task protocol followed by prior multi-task learning work (Liu et al., 2023; Navon et al., 2022).

Model. Just as with NYU-v2, the model architecture used in our experiments is a Multi-Task Attention Network (MTAN) (Liu et al., 2019) built on top of SegNet (Badrinarayanan et al., 2017). The network takes an RGB image

²<https://github.com/AvivNavon/nash-mtl>

³<https://github.com/Cranial-XIX/FAMO>

Table 5. Hyperparameters used for MT10 (v1) SAC.

Component	Value
Encoder feature dim	50
Discount γ	0.99
Initial temperature α_0	1.0
Actor update freq.	1 step / env step
Critic target τ	0.005
Target update freq.	1 step / env step
Encoder EMA τ_{enc}	0.05
Learning Rate	0.025
Update-weights cadence	every step (= 1)

as input and produces two task-specific outputs via separate heads: (i) a per-pixel class-score map for semantic segmentation, (ii) a scalar depth map for depth estimation. For LS, MGDA, UW, FAMO, NashMTL, IGBv2, and DiBS-MTL, we use the multi-task attention network (MTAN) (Liu et al., 2019) with a SegNet-style encoder-decoder architecture and apply the same training schedule, optimizer, and data-augmentation procedures as established in prior work for a fair comparison. For LDC (Xiao et al., 2025) and GO4Align (Shen et al., 2024), we use the task architectures provided in their original implementations.

Training Protocol. We follow the procedure outlined in (Navon et al., 2022). We train for 300 epochs with Adam (Kingma & Ba, 2014), using an initial learning rate of 1×10^{-4} reduced to 5×10^{-5} after 100 epochs. All reported results are averaged over three random seeds, namely 1, 7, and 42.

E.4. QM9

Benchmark and Setup. The QM9 dataset (Blum & Reymond, 2009) is a graph neural network learning benchmark consisting of 11 tasks, and is a widely used challenging benchmark in MTL literature (Navon et al., 2022; Liu et al., 2023; Xiao et al., 2025; Dai et al., 2023; Shen et al., 2024). It consists of molecules represented by annotated graphs. Our experimental setting is the same as that used in prior MTL works, and the tasks are to predict 11 different molecular properties.

Model. Following Navon et al. (2022), we use the PyTorch Geometric implementation of Fey & Lenssen (2019), which incorporates the widely used GNN architecture of Gilmer et al. (2017) together with the pooling operator of Vinyals et al. (2015). As with the other benchmarks, LDC and GO4Align use their own architectures.

Training Protocol. We train each method for 300 epochs and perform a learning-rate search based on the validation Δm metric. A learning-rate scheduler reduces the learning rate once the validation Δm stops improving, and the validation set is additionally used for early stopping. All reported results are averaged over three random seeds, namely 1, 7, and 42. This is in line with the approach taken by (Navon et al., 2022).

E.5. Meta-World MT10

Benchmark and Setup. The MetaWorld MT10 (v1) benchmark comprises ten robotic manipulation tasks: Reach, Push, Pick-and-Place, Door Open, Drawer Open, Drawer Close, Button Press (Top-Down), Peg Insert, Window Open, and Window Close (Yu et al., 2020b). Each task has distinct reward functions and success criteria. We build on the MTRL code base (Sodhani & Zhang, 2021)⁴ with MetaWorld⁵.

Policy and Training Protocol. We train a single Soft Actor-Critic (SAC) policy shared across all ten tasks. multi-task learning (MTL) methods are applied to balance the actor and critic updates within the shared SAC. For each MTL method, we train for 2,000,000 environment steps in total. Episodes have length 150; this corresponds to $\approx 13,333$ episodes overall.

⁴<https://github.com/facebookresearch/mtrl>

⁵<https://github.com/Farama-Foundation/Metaworld>

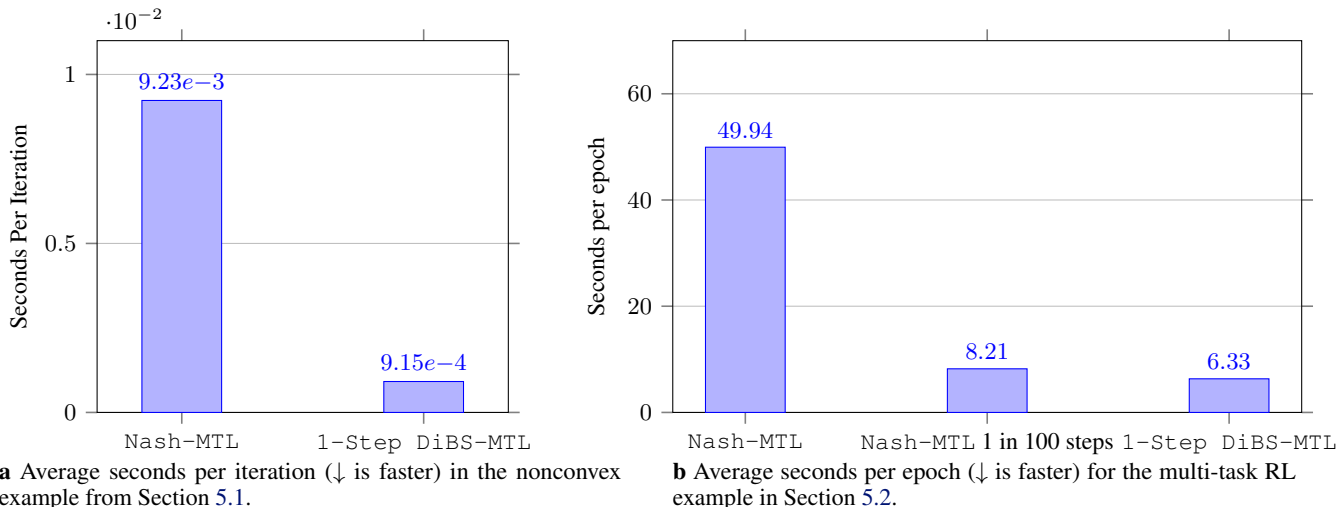


Figure 4. Runtime comparisons across nonconvex demonstrative example and multi-task RL settings.

Table 6. Run times in minutes (\downarrow is faster) for supervised MTL experiments in Section 5.3 averaged over 3 seeds.

	Benchmarks		
	NYU-V2	Cityscapes	QM9
1-step DiBS-MTL	819.33	481.67	1705
5-step DiBS-MTL	1713	612	1719
10-step DiBS-MTL	1799	752	1726
Nash-MTL	1031	598	1699

Evaluation is performed every 200 episodes (30,000 steps) on all tasks, and reported metrics are averaged over 10 random seeds: 1, 2, 3, 4, 5, 6, 7, 8, 9, 10.

Hyperparameters. Key hyperparameter values are provided in Table 5. We follow the same hyperparameters defined in prior works (Navon et al., 2022; Liu et al., 2023; 2021a; Ban & Ji, 2024).

Reproducibility Note. During preliminary experiments, we observed that using the same random seed did not always produce identical training curves. This discrepancy arose because the original MTRL code (Sodhani & Zhang, 2021) did not seed the initial action sampling during the exploration phase. As a result, small differences in early exploratory actions (first 10 steps) propagated through training and produced slight variation in learning behavior even with fixed seeds.

F. Additional Results

F.1. Comparison of DiBS-MTL runtimes with previous bargaining MTL method Nash-MTL.

We also evaluated the computational speed of the DiBS-MTL with the previous bargaining-inspired MTL method, Nash-MTL. Specifically, we compare runtimes of DiBS-MTL with Nash-MTL for the demonstrative nonconvex examples (Figure 4), the multi-task reinforcement learning example (Figure 4), and the supervised learning NYU-V2, QM9 and Cityscapes examples (Table 6).

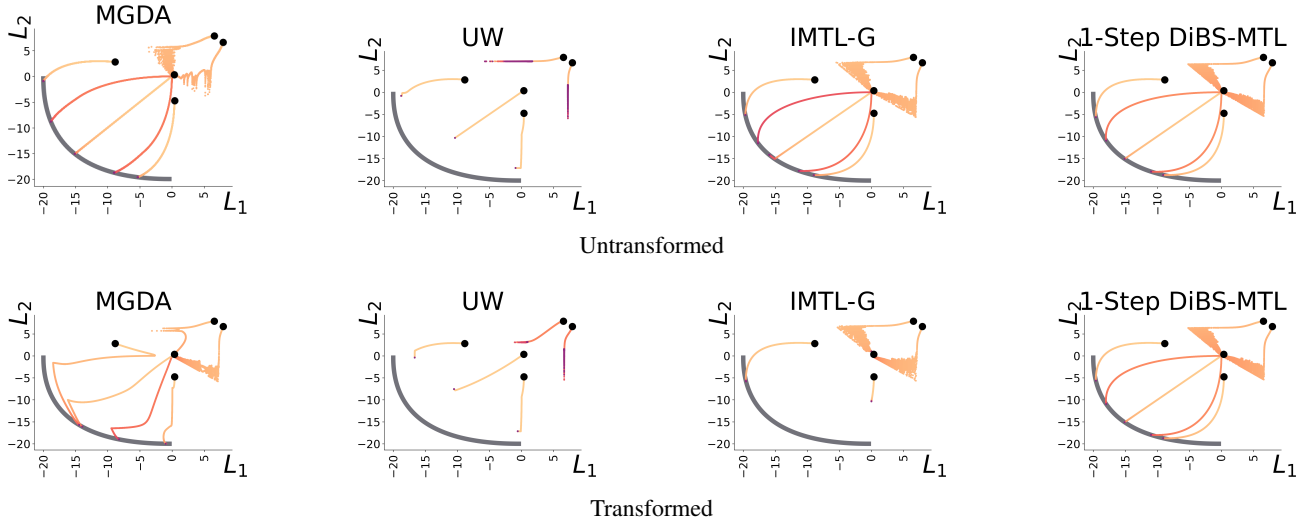


Figure 5. Additional experiments performed in the demonstrative two-objective example. We observe that `1-step DiBS-MTL` exhibits the same invariance to monotone non-affine transforms as `T-step DiBS-MTL` from Figure 2, and also demonstrates similar behaviour, tracing very similar trajectories as `T-step DiBS-MTL` ($T = 5$) from the same initializations.

Algorithm 2 DiBS-MTL Single Step

Require: Initial parameters $\theta_{(0)}$, losses $\{\ell^i\}_{i=1}^N$, learning rate η , number of epochs J

for $j = 1$ to J **do**

Compute task gradients $\nabla_{\theta_{(j-1)}} \ell^i$

Compute DiBS update direction:

$$d_{(j)} = \sum_{i \in [N]} \frac{\nabla_{\theta} \ell^i(\theta_{(j-1)})}{\|\nabla_{\theta} \ell^i(\theta_{(j-1)})\|_2}$$

Update: $\theta_{(j)} \leftarrow \theta_{(j-1)} - \eta d_{(j)}$

end for

return $\theta_{(J)}$

From Figure 4, it is clear that DiBS-MTL consistently is faster than Nash-MTL for the demonstrative nonconvex and the multi-task reinforcement learning examples. In the multi-task reinforcement example particularly, Nash-MTL is particularly slow if applied for every training iteration, and even when applied only once per 100 training loops (which is the speedup suggested by the original authors (Navon et al., 2022)), it is still slower than `1-step DiBS-MTL`. We conjecture that the slow performance of Nash-MTL is because it solves a separate convex optimization problem at each iteration which is time consuming.

In Table 6, we compare the runtime of different DiBS-MTL variants and Nash-MTL across the MTL benchmarks to assess how the number of bargaining steps affects computational cost. The single-step version of DiBS-MTL achieves the fastest runtimes on NYU-V2 and Cityscapes, while falling slightly behind Nash-MTL on QM9. As expected, runtime for DiBS-MTL variants increases as the number of steps increase, because the per epoch complexity increases, reflecting the added cost of performing multiple bargaining updates. At the same time, as indicated by Tables 2 to 4, `1-step DiBS-MTL` achieves comparable performance to the multi-step versions, making `1-step DiBS-MTL` an appropriate approximation of multi-step DiBS-MTL variants.

F.2. Additional Results in the Demonstrative Nonconvex Example

In addition to the results reported in section Section 5.1, we also ran additional methods in the demonstrative two-objective example. Specifically, we ran the Multiple Gradient Descent Algorithm (MGDA) (Désidéri, 2012), Uncertainty Weighting (UW) (Kendall et al., 2018), Impartial Multi-task Learning (IMTL-G) (Liu et al., 2021b), and `T-step DiBS-MTL`. We run `T-step DiBS-MTL` for 10 steps per update. The loss functions and number of steps are identical to the experiment described in Section 5.1.

In Figure 5, we observe that the additional baseline methods of MGDA, UW, IMTL-G are not invariant to the transform, with UW failing to reach the Pareto-front in both cases. We note that `T-step DiBS-MTL` performs similarly to single step DiBS-MTL. `T-step DiBS-MTL` reaches the same points on the Pareto-front in both cases, showing it is also invariant to monotone non-affine transforms.

G. 1-step DiBS-MTL Algorithm Pseudocode

Algorithm 2 provides pseudocode for the `1-step DiBS-MTL` algorithm. When adapting DiBS-MTL to the single-step variant, the distances to the preferred states for each agent are equal. For `1-step DiBS-MTL`, for all j in Algorithm 1, $\|\theta_{(j-1)} - \theta^{*,i}\| = \epsilon$ for all i . The approximation radius ϵ and the step size η_s are absorbed into the learning rate η .